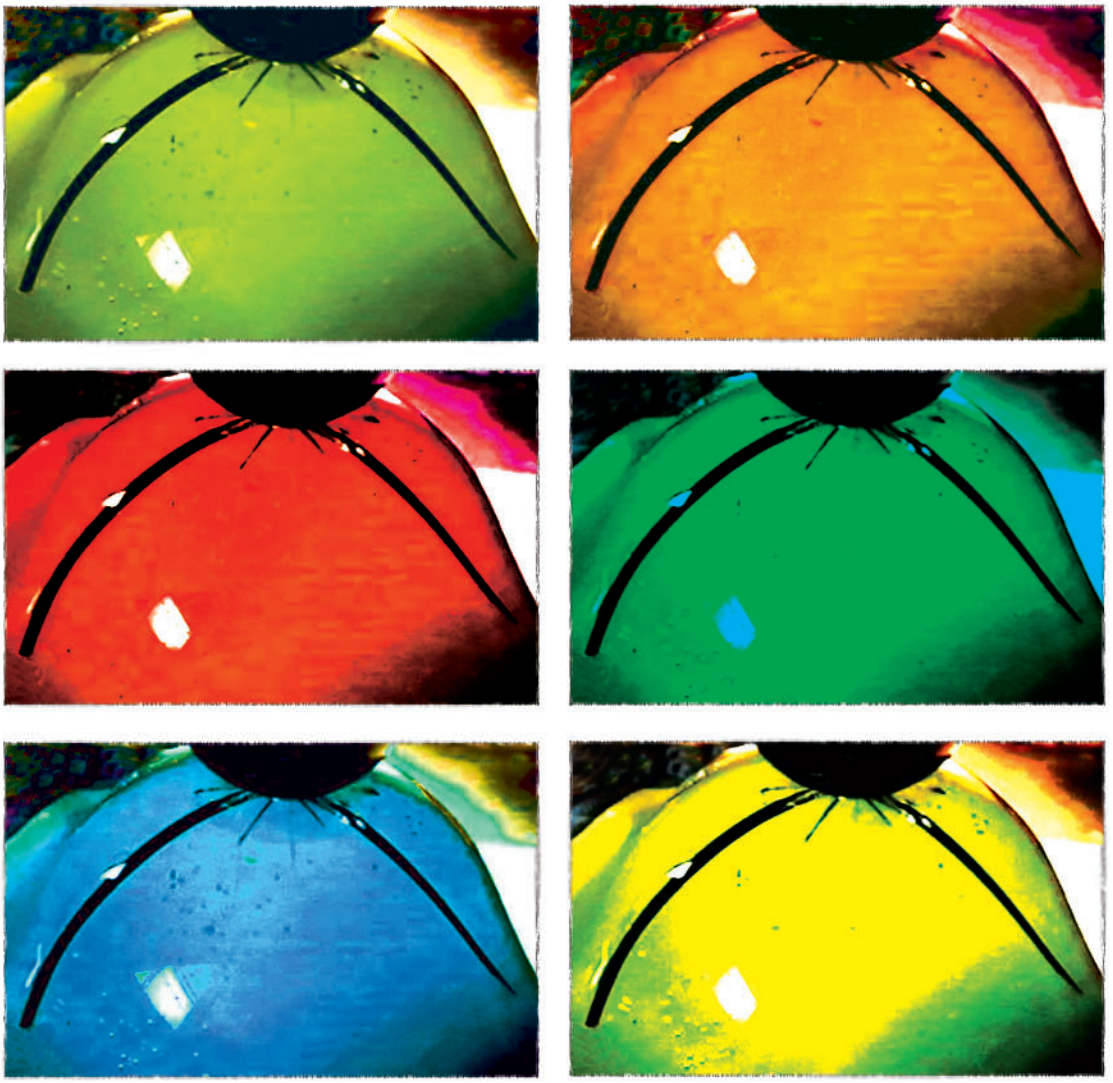

Journal of the American Ceramic Society

Volume 88 Number 8 August 2005

journal

J. Am. Ceram. Soc., **90** [6] 1671–1683 (2007)
DOI: 10.1111/j.1551-2916.2007.01585.x
© 2007 The American Ceramic Society
No claim to original US government works

Failure Modes in Ceramic-Based Layer Structures: A Basis for Materials Design of Dental Crowns

Brian Lawn[†] and Sanjit Bhowmick

Materials Science and Engineering Laboratory, Ceramics Division, National Institute of Standards and Technology, Gaithersburg, Maryland 20899-8520

Mark B. Bush and Tarek Qasim

School of Mechanical Engineering, The University of Western Australia, Crawley, Western Australia 6009, Australia

E. Dianne Rekow and Yu Zhang

New York University College of Dentistry, 345 East 24th Street, New York, New York 10010

A research program on failure modes induced by spherical indenters in brittle layer structures bonded to polymeric substrates, in simulation of occlusal function in all-ceramic dental crowns, is surveyed. Tests are made on model flat and curved layers bonded onto a dentin-like polymer base, in bilayer (ceramic/polymer) and trilayer (ceramic/ceramic/polymer) configurations. All-transparent systems using glass as a porcelain-like outer or veneer layer and sapphire as a stiff and strong core support layer enable *in situ* observation of the entire evolution of fracture modes in the brittle layers, from initiation through to failure. With the fracture modes identified, tests are readily extended to systems with opaque polycrystalline dental core ceramics, notably alumina and zirconia. A variety of principal failure modes is identified: outer and inner cone cracks developing in the near-contact region at the top surface; radial cracks developing at the bottom surface along the loading axis; margin cracks from the edges of dome-like structures. All of these modes are exacerbated in cyclic loading by time-cumulative slow crack growth, but inner cones are subject to especially severe mechanical fatigue from hydraulic pumping of water into the crack fissures. Conditions under which each mode may be expected to dominate, particularly in relation to geometrical variables (layer thickness, contact radius) and relative material properties, are outlined. Clinical issues such as crown geometry, overload versus fatigue failure, role of residual stresses in fabrication, etc. are addressed.

D. Green—contributing editor

Manuscript No. 22546. Received December 4, 2006; approved January 10, 2007.
This work was supported by a grant from the National Institute of Dental and Craniofacial Research (PO1 DE10976) and by the Australian Research Council.
[†]Author to whom correspondence should be addressed. e-mail: brian.lawn@nist.gov

I. Introduction

Ceramic materials are now widely used in biomechanical replacements and restorations—dental crowns, hip and knee prostheses, spinal disks, heart valves, bone implants, and so on—where strength, wear resistance, bioinertness, and chemical durability are defining issues. Biomechanical prostheses usually include more than one material type—ceramic, metal, polymer—commonly in some layer or other composite configuration. Because of their brittleness, ceramic components demand particular attention in system design. Yet, despite a pervasive incidence of prosthesis failures in patients, the materials limitations of such devices remain poorly understood by practitioners, where studies are dominated by clinical trials and analysis of retrievals. Most prostheses are characterized by a complexity of configurational geometries and concentrated loads, and are subject to millions of cycles in body fluids. The challenge for the ceramic scientist is to develop materials that will withstand such exacting conditions over extended lifetimes. Considerable effort has been made to provide a scientific basis for understanding the role of materials properties in ceramic-based layer structures by testing model systems in simple contact force conditions simulating the basic elements of biomechanical load-bearing function. What is emerging is a host of competing failure modes that need to be understood in relation to underlying material properties (modulus, strength, and toughness) and geometrical factors (characteristic contact dimension, layer thickness).[1–3]

Nowhere is the need to understand the mechanics of failure more evident than in the design of ceramic-based dental crowns and restorations.[4–18] Crown placement is by far the most widespread of all prosthetic procedures, amounting to an annual billion dollar industry. Ceramics are materials of choice for crowns because of an increasing demand for esthetics in the mouth, as well as for bioinertness. Typically, molar crowns, where chewing stresses are highest, must be designed to withstand biting loads of 100–1000 N for more than a million cycles

Feature

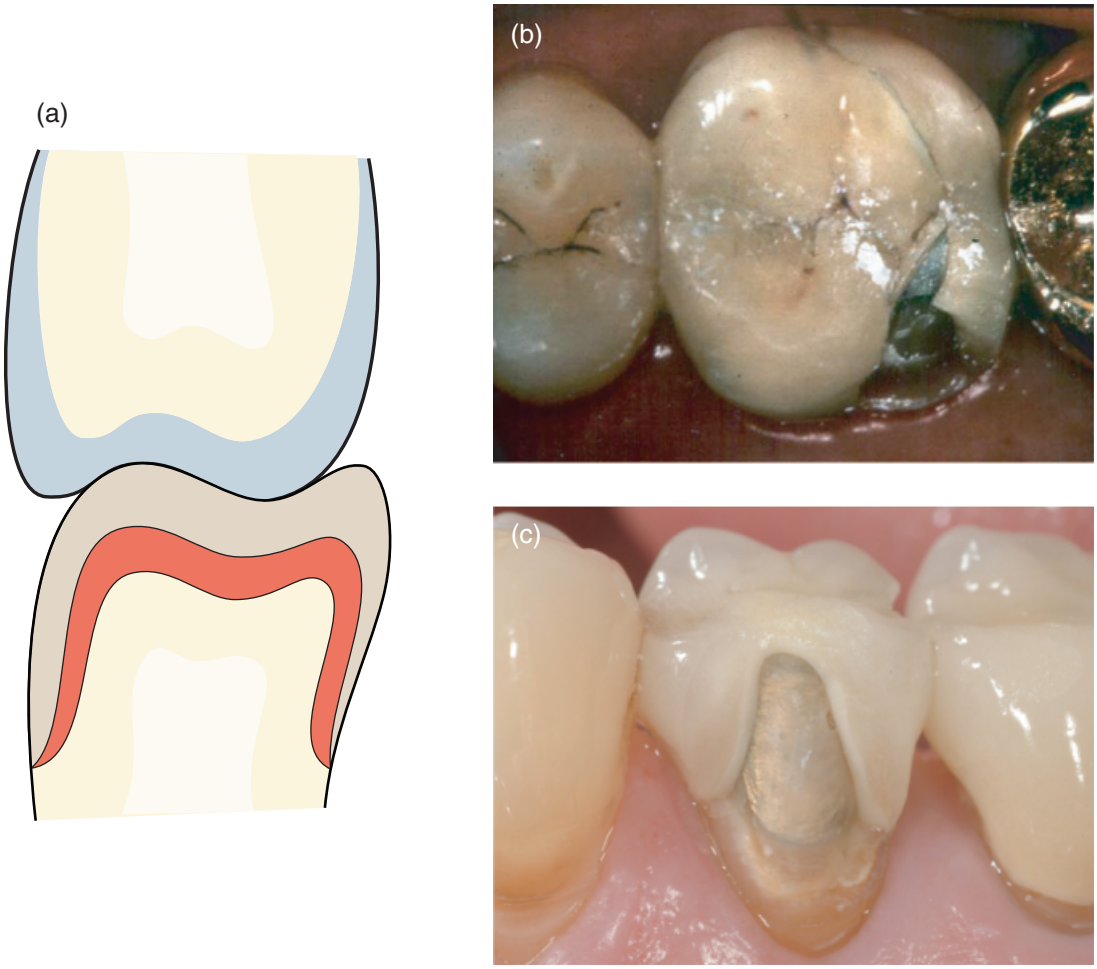

Fig. 1. Fracture of all-ceramic dental crowns. (a) Schematic showing essential trilayer structure of porcelain-fused-to-ceramic crown on dentin. (b) Occlusal failure of InCeram (porcelain/alumina) crown (courtesy Suzanne Scherrer). (c) Margin or semi-lunar failure of Dicor (glass-ceramic) crown (courtesy Kenneth Malament).

in aqueous environments.[10,18,19] Their net thickness, decided for the most part by the remaining tooth structure as well as by geometrical constraints from the adjacent and opposing dentition, ranges from around 1.5 to 2 mm near the top contact surface down to around 1 mm or less near the margins. The characteristic occlusal contact radii, as measured from tooth sections, range from 1 to 10 mm. The earliest ceramic crowns were effectively bilayer structures fabricated from single glass–ceramic or high-leucite porcelain layers and bonded directly onto underlying soft tooth dentin. However, these structures revealed unacceptably high failure rates.[13,17] Subsequently, the most common all-ceramic crowns have taken on the form of an esthetic porcelain veneer fused onto a stiff, hard, strong ceramic core—alumina or zirconia. The resultant structure is effectively a trilayer, with the brittle veneer/core crown seated onto the tooth dentin (Fig. 1(a)). The stiff core provides, among other benefits, stress-shielding of the weak veneer layers as well as of the underlying soft dentin support. Although a marked improvement over monolithic crowns, veneer/core systems on posterior teeth still fail at a higher rate than their traditional porcelain-fused-to-metal counterparts,[16,20] with fractures originating in both veneer and core. Two reported failure types are shown in Fig. 1: fracture at the occlusal contact region (Fig. 1(b)); and "semi-lunar" fractures on the crown side wall (Fig. 1(c)). However, clinical data are limited and the issue of failure origins remains somewhat controversial in the dental community.

Materials engineering has an important role to play in understanding these kinds of fractures and how to counteract them. To quote a passage from the Introduction to a recent text on Dental Functional Morphology by Peter Lucas (professor of anatomy and anthropology no less):[19] " … How do teeth work? One relatively uniform answer is provided in numerous accounts in top journals and even school texts. It is that teeth

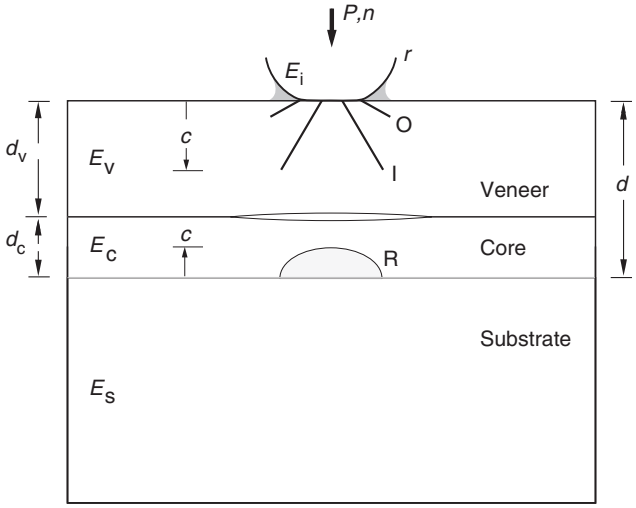

Fig. 2. Schematic diagram for model flat veneer/core layer structures loaded with spherical indenters for evaluating fracture modes: O, outer cone cracks; I, inner cone cracks; R, radial cracks. Delamination cracks at veneer/core interface, as well as radial cracks at veneer bottom surface and median cracks within near-contact quasiplasticity zones (not shown), are secondary modes.

variously crush, cut, shear or grind food. That is more or less the prevailing wisdom in dentistry, zoology, paleontology, anthropology and many other biological fields … Despite apparent unanimity, these accounts are completely wrong. **A genuine account of tooth function … starts in the still obscure world of fracture mechanics** … ." Lucas explains how oral health is vital to the survival of all animals, including humans, and how tooth function has played a central role in the evolution of species. From the ceramics engineering standpoint, the question then arises as to how we may use fracture mechanics as a characterization tool to design superior crowns in order to restore dental function in humans. Answering this question is a goal of the present article.

Accordingly, we review some of the more recent results from contact loading tests in our laboratories on structures containing one or two brittle layers on a compliant base, i.e., bilayers or trilayers.[1–3,21–53] Bilayers provide a sound starting point for establishing fracture mechanics relations for the more complex (and, arguably, more clinically relevant) case of trilayers. These structures are especially vulnerable to high-intensity (occlusal) contact stresses at the top veneer surface and flexural stresses at the bottom core surface. In their simplest form, they are fabricated as flat-layer structures, with sphere (Hertzian) contact loading, as indicated in Fig. 2, although more recent work is progressing into dome-like structures more representative of actual tooth geometry. Model transparent materials—glass (representing porcelain veneer), sapphire (representing ceramic core), and polycarbonate (representing support dentin)—enable direct viewing of fracture modes during loading using video cameras. An additional advantage of these model structures is that surfaces can be selectively abraded to produce controlled starting flaws for crack initiation, thereby opening the way for preselecting the source of the dominant fracture mode. For instance, abrasion with a slurry of SiC particles produces flaws of size 10–20 μm.[22] Tests have also been conducted on a variety of opaque, polycrystalline crown ceramics and dentin-like support materials. Several fracture modes have been identified in such tests, but those considered most likely to result in failure are outer (O) and inner (I) cone cracks within the veneer in the near-contact field and radial cracking (R) within the core in the flexural far field. Interfacial delamination cracks appear to be secondary in most systems studied, as are radial cracks that initiate at the bottom surface of the veneer and median cracks within near-contact quasiplasticity zones (not shown). The often complex competition between these modes *en route* to failure may not always be evident from routine *postmortem* fractography. The very term "failure" is subjective—here, we define it as the point at which a crack traverses the layer in which it initiates. Issues such as crack prevention versus crack containment, flat versus curved specimen surfaces, single-cycle overload fracture versus long-term multi-cyclic fatigue fracture, materials fabrication (including role of residual stresses), will be addressed. In the case of fatigue, the role of water in generating mechanical driving forces, in addition to slow crack growth, will be highlighted.

II. Bilayers

(1) Flat Layer Structures

Begin with flat bilayer structures of plate thickness d loaded with a sphere of radius r at normal load P over number of cycles n. This is a special case of Fig. 2 in which the veneer/core system is replaced with a monolithic ceramic without internal interface ($d_c = 0$, $d_v = d$). These simplistic structures enable identification of basic fracture modes with minimum complication. A feature of the bilayer structure is the manner in which the relative values of r and d determine the nature of dominant stress fields[54]: for large d and small r, the tensile stresses concentrate outside the contact in the ceramic top surface and have the form of the classical Hertzian stress field,[55]

$$\sigma \sim (P/r^2)^{1/3} E_v^{2/3} \tag{1}$$

highlighting contact radius dependence; for small d and large r, the tensile stresses are transferred to the ceramic bottom surface and assume the form of a flexing plate on a compliant substrate,[22]

$$\sigma \sim (P/d^2) \log(E_v/E_s) \tag{2}$$

highlighting layer thickness dependence. Note the appearance of the core ceramic and substrate modulus terms E_v and E_s in Eqs. (1) and (2).

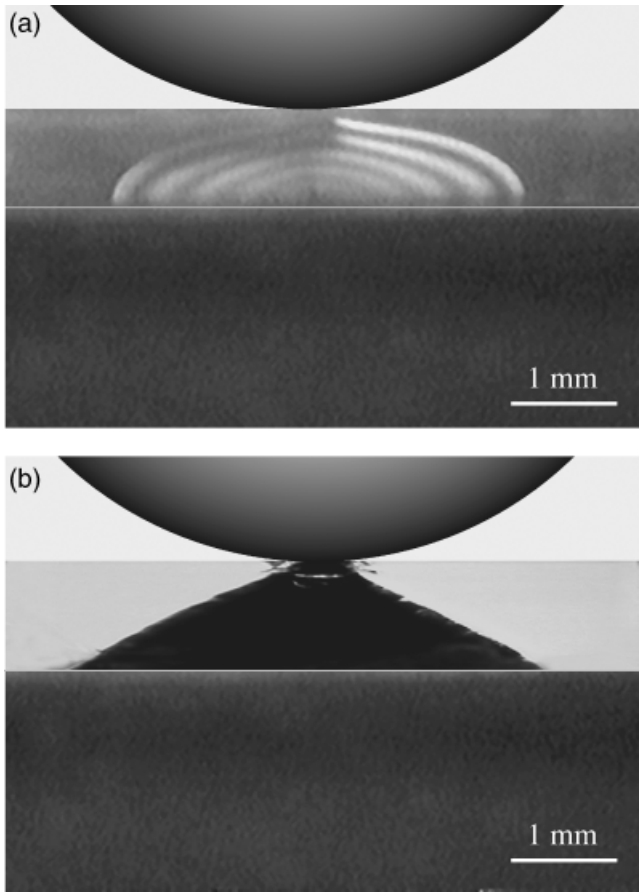

Fig. 3. Side views of cracks in soda-lime glass layer, $d = 1.0$ mm, on polycarbonate polymer substrate, indenter with tungsten carbide sphere. (a) Showing R crack initiated at abraded bottom surface, single-cycle load $P = 130$ N, sphere radius $r = 4.0$ mm, in air. Fizeau fringes are from light interference at crack walls. After Chai *et al.*[22] (b) Showing I crack initiated at abraded top surface, peak cyclic load $P_m = 150$ N at frequency 1 Hz, $r = 1.6$ mm, $n = 228$ cycles, in water. Preceding O crack barely visible at top surface. (Interfaces accentuated by superimposed white lines for clarity.) After Bhowmick *et al.*[38]

Figure 3 shows side-view *in situ* photographs of cracks in glass layers of thickness $d = 1$ mm bonded onto a polycarbonate base with a thin layer of epoxy resin and indented with tungsten carbide (WC) spheres. In Fig. 3(a), the specimen is abraded at the glass bottom surface (top surface etched) and subjected to a single cycle.[22] At a threshold load, a radial crack initiates at the interface and spreads upward and sideways in the glass. Increasing the load causes the crack to multiply into several arms and to continue to spread sideways in radial directions. Higher loads are required to drive the crack to the top surface (see later). Cycling at a well-defined peak load simply reduces the threshold for initiation and causes the crack to spread steadily over extended time.[32] Such rate-dependent growth is attributed to slow

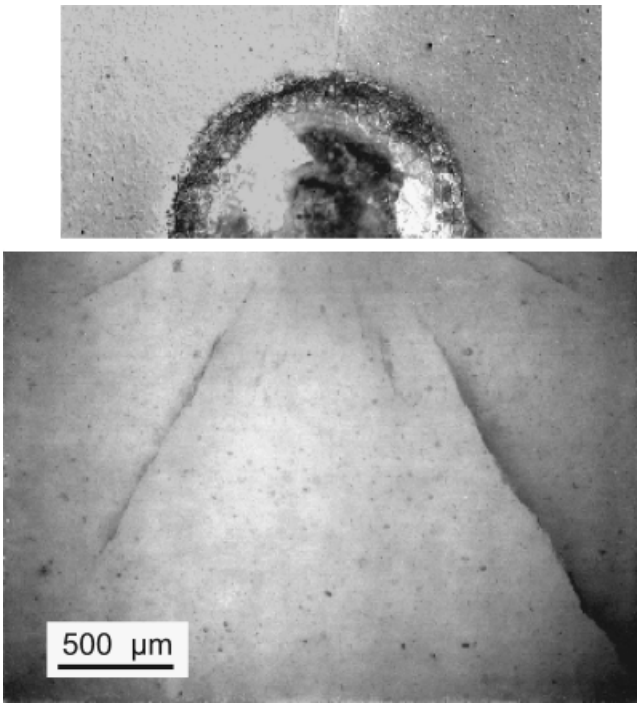

Fig. 4. Half-surface and side-section views of cone cracks in porcelain monolith, peak cyclic load $P_m = 500$ N, $r = 3.18$ mm, $n = 510$ cycles, frequency 10 Hz, in water. Shallow O cracks and deep I cracks form beneath the near-surface damage zone. After Kim *et al.*[67]

crack growth due to incursion of moisture from the polymeric adhesive at the glass/substrate interface. As a rule of thumb, the effect of slow crack growth is to diminish the critical loads to initiate radial cracks by a factor of 2 or 3 over an integrated contact duration of a year or more.[36,56]

Figure 3(b) corresponds to the same specimen but with abrasion at the glass top surface (bottom surface etched). An inner (I) cone crack has initiated within the maximum contact circle at the top surface and propagated steadily through the glass to failure. A distinguishing characteristic of such I cracks is that they occur only in cyclic loading in liquid. They propagate considerably more steeply than their companion outer (O) cone cracks (in this case barely visible at the top surface). The geometrical relation between outer and inner cone cracks is seen more clearly in Fig. 4, a section through a monolithic dental porcelain specimen after a similar cycling history. This latter example confirms the generality of the cone crack geometry in brittle materials. (Note, however, a somewhat less steep descent of the inner cones in Fig. 3(b) relative to Fig. 4, attributable to modification of the stress field from the superposition of a flexural stress component in the bilayer relative to the monolith.[57]).

In such transparent bilayer specimens, the growth characteristics are readily characterized by *in situ* monitoring of the crack depth c during extended testing (Fig. 2). Figure 5 shows c as a function of number of cycles n for each crack type in cyclic loading of preferentially abraded glass plates of thickness $d = 1.5$ mm in water, for a sphere of radius $r = 1.6$ mm.[38] The load form is haversinusoidal, frequency 1 Hz, with minimum load 2 N (to prevent the indenter wandering over the surface). At the peak load $P_m = 200$ N represented in these tests, outer cone (O) cracks initiate within the first cycle and grow steadily with continued cycling. Inner cone (I) and radial (R) cracks initiate much later. The growth rates of O and R cracks are entirely consistent with slow crack determined by a classical crack velocity relation. Despite their delayed initiation, the I cracks rapidly outgrow their competitors *en route* to penetration of the glass layer. This is indicative of some additional, mechanical driving force, in combination with a superposition of flexural tensile stresses in the lower half of the glass plate. Which of the various crack types causes ultimate failure in any given material

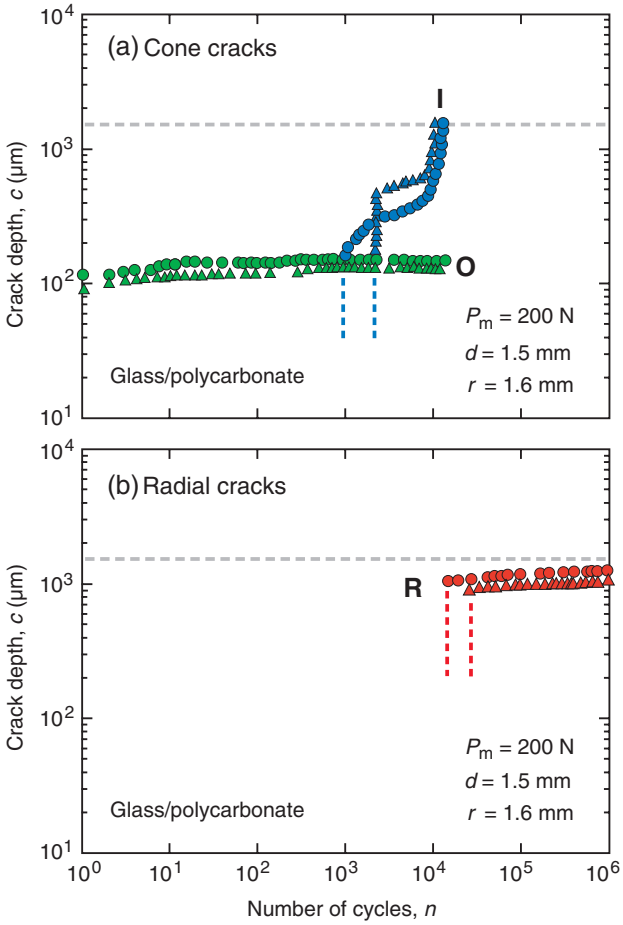

Fig. 5. Crack depth c for bilayers of glass thickness $d = 1.5$ mm (dashed lines) on polycarbonate base, as function of number of cycles n for indentation with tungsten carbide sphere of radius $r = 1.6$ mm, peak load $P_m = 200$ N, frequency 1 Hz, in water: (a) O and I cone cracks, glass top surface abraded, (b) R cracks, glass bottom surface abraded. Each symbol represents a separate test. Vertical dashed lines indicate initiation.

system can vary, depending on the peak load as well as surface abrasion conditions (as we shall demonstrate later in connection with trilayer systems). Following on from Eqs. (1) and (2), we find that cone cracks dominate in bilayers with large d and small r, radial cracks in specimens with small d and large r.

The nature of the mechanical force driving the I cracks in cyclic loading in water warrants elaboration, because it is a fairly recent addition to the fracture mechanics repertoire.[42] Recall from Fig. 5 that such cracks are not evident at all during single-cycle loading, indeed not until after several hundreds of cycles. These I cracks form at approximately one-half the radius of the outer cone (Fig. 4). Figure 6 depicts the mechanism of formation. The stress field within an approximate hemispherical zone below the contact is strongly compressive, mildly tensile outside. Generally, an O crack forms first, often during the initial cycle. On subsequent cycling, the approaching contact opens up surface flaws within the maximum contact zone and allows minute volumes of water to enter (Fig. 6(a)). As the contact engulfs and closes the mouths of the fissures, the trapped water is squeezed to the crack tip regions, driving the cracks incrementally downward (Fig. 6(b)). On the next cycle, the volume of water entering the fissures is slightly larger, and so the fatigue process builds up slowly but inexorably, ultimately resulting in full-scale penetration in Fig. 3(b). Flaws about halfway between the center and the maximum contact circle provide favored locations for a maximum squeezing effect. We re-emphasize the essential role of liquid in the squeezing process, as evidenced by the absence of I cracks for tests in air. Note also that O cracks form outside the contact, and are therefore immune to such mechanical fatigue,

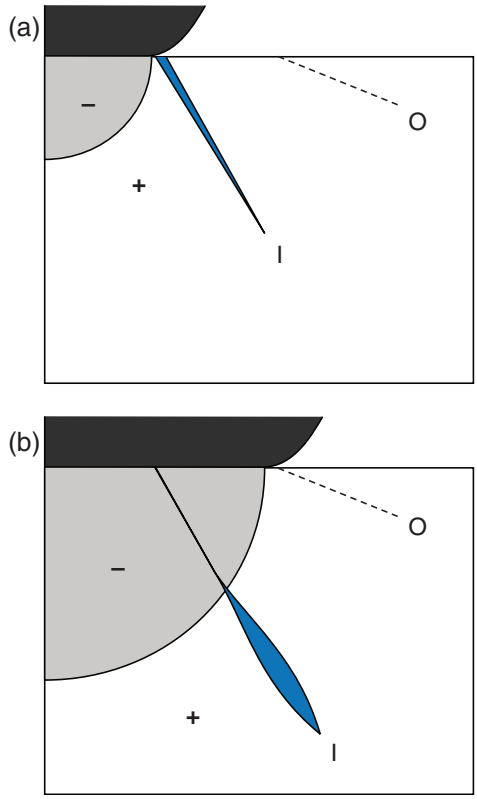

Fig. 6. Illustrating the hydraulic pumping mode of I crack propagation. On successive cycles, the expanding contact opens up fissures at the top surface, (a) first allowing water to enter the mouths within the tensile field and (b) then squeezing the water to the tip regions. The process is cumulative, resulting in mechanical fatigue.

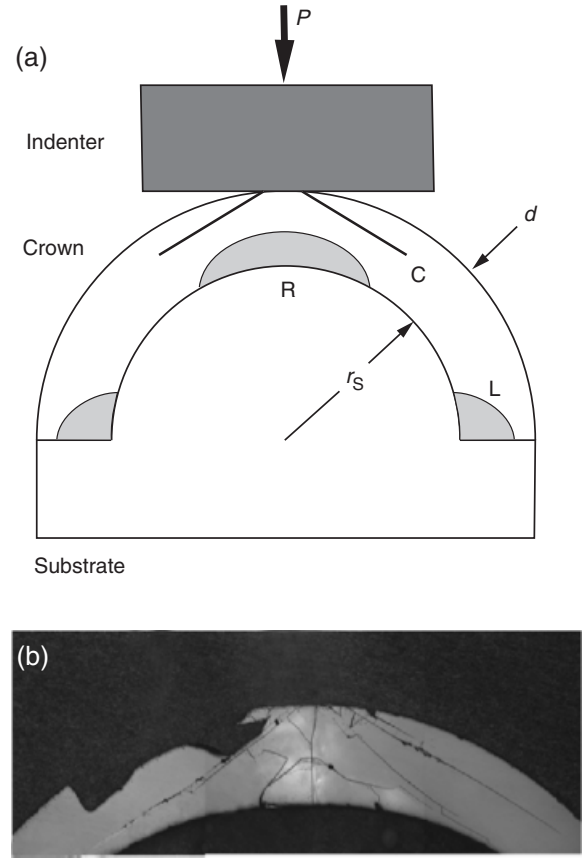

Fig. 7. Section profile of failed glass dome specimen of thickness $d = 1$ mm backfilled with substrate of modulus $E_s = 15$ GPa. Flat disk steel indenter, overloaded to $P = 820$ N. Traces of radial cracks and cone cracks with extensive spalling are apparent. After Kim *et al.*[51]

regardless of the environment. The mechanics of the complex hydraulic pumping process have been confirmed by numerical simulation using finite element analysis.[39,57]

This description of fracture modes captures the simplest elements of the competing failure processes in bilayer structures. It ignores other damage modes. For instance, median cracks can be generated immediately below the indenter in less brittle ceramics by quasiplasticity processes.[43,58] As with hydraulic pumping, median cracks are subject to mechanical fatigue, from progressive accumulation of stresses within the quasiplastic damage zone. In this sense, although arising from a different source, median cracks have common characteristics with the inner cones. Then there is the issue of delamination at the ceramic/substrate interface. In most experimental setups examined in our work delamination is, at worst, a secondary fracture mode, occurring only after penetration of one or other of the cone or radial cracks through the brittle layer in which they initiated. All that is needed to avoid premature delamination is to ensure an adequately strong bond, a condition comfortably met by the epoxy resins used to join the layers in Figs. 3 and 4. Some dental cements, however, do not necessarily meet this minimum requirement, in which case delaminations can occur first, with enhanced transverse failure.[35]

Extensive fracture mechanics modeling has been conducted for bilayer systems, enabling calculation of critical conditions for crack initiation and layer failure in terms of material properties, including crack velocity exponents, and governing geometrical variables, notably plate thickness d and occlusal radius r.[22–24,28,30,32,34,38,39,43,59–61] Such modeling provides an essential first step for later consideration of trilayers.

(2) Curved Layer Structures

Now consider the effect of introducing curvature to bilayer surfaces. This takes us one step closer to real crown structures. Figure 7(a) illustrates such a configuration, a brittle dome of thickness d and inner radius r_s with compliant interior. This figure depicts a flat indenter on a curved specimen, i.e., an inversion of the traditional Hertzian contact problem, although a more general case is a sphere on sphere. Experimentally, the dome shells are most readily produced by allowing glass plates to slump over a steel ball die at the glass softening temperature, and then backfilling the resultant shells with epoxy (similar modulus to polycarbonate).[40] The fracture modes in the vicinity of the contact remain more or less the same—cone (C) and radial (R) cracks. A section through the contact region of glass dome indented with a steel disk, Fig. 7(b), illustrates how such cracks can traverse the thickness and cause serious spallation.[51]

To illustrate the role of specimen curvature on failure characteristics, Fig. 8 compares radial crack patterns from single-cycle indentations of (a) flat ($r_s = \infty$) and (b) dome ($r_s = 8$ mm) specimens of the same thickness ($d = 1$ mm) with a metal sphere ($r = 4$ mm) at a common load ($P = 1500$ N).[40] In both cases the glass surfaces were abraded at their bottom surfaces before epoxy backfilling, so favoring radial cracks. The crack patterns are highlighted by judicious backlighting. In the case of the domes, the radial cracks have broken through to the top surface, at which point they have become unstable and propagated abruptly to the dome margins. It is clear that specimen curvature has enhanced failure.

The mechanics of crack evolution in curved structures is complex, and in the case of radial cracking requires three-dimensional (3D) analysis. Figure 9, constructed from boundary element analysis (BEA), indicates how radial crack profiles evolve with increasing load in epoxy-backfilled glass domes.[41] In these calculations, the cracks are allowed to grow incrementally, at each step adjusting the profile to equilibrate the stress intensity factor along each crack front. Breakthrough of the crack to the top surface, at which point the crack front

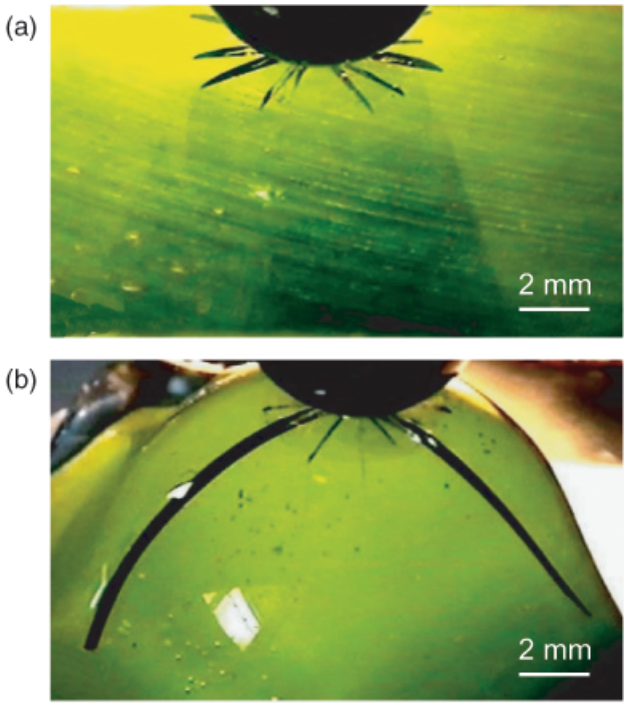

Fig. 8. Radial cracks in glass layer of thickness $d = 1$ mm with abraded undersurface backfilled with epoxy resin, from loading with tungsten carbide sphere of radius $r = 4$ mm at load $P = 1500$ N: (a) flat surface, $r_S = \infty$, (b) curved surface, $r_S = 8$ mm. After Qasim *et al.*[40]

straightens into failure instability, occurs over shorter propagation distances with increasing specimen curvature. BEA predictions of the critical loads P_F to take the radial cracks for glass domes of thickness $d = 1$ mm to breakthrough are plotted in Fig. 10 as the solid curve as a function of surface curvature, along with data from experimental observations of the failure condition for abraded and unabraded shells. Note that the failure condition is not sensitive to the original flaw state, being determined primarily by the flexural stress conditions in the lower half of the glass plate. Included as the dashed lines are predicted loads P_I to initiate these same cracks (equating maximum tensile stress at bottom surfaces of shells to strengths of abraded and unabraded glass). Whereas the loads P_F diminish strongly with increasing curvature, the corresponding loads P_I

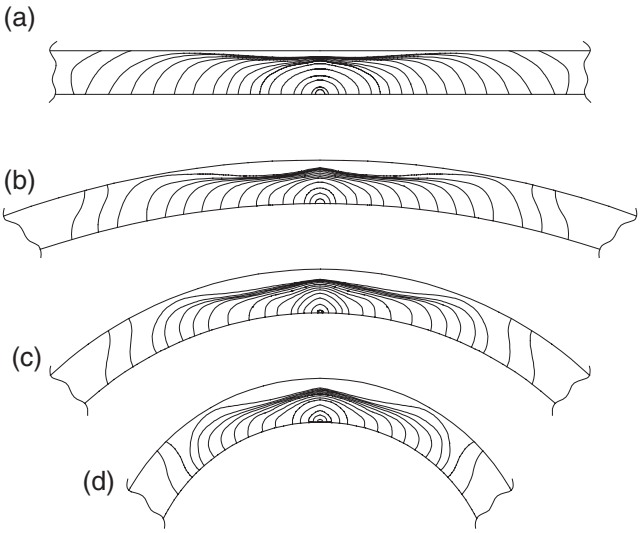

Fig. 9. Boundary element analysis-calculations of radial crack evolution through brittle dome-like glass layers of different curvatures on epoxy backing: (a) $r_c/d = \infty$ (flat), (b) $r_c/d = 20$, (c) $r_c/d = 8$, (d) $r_c/d = 4$. After Rudas *et al.*[41]

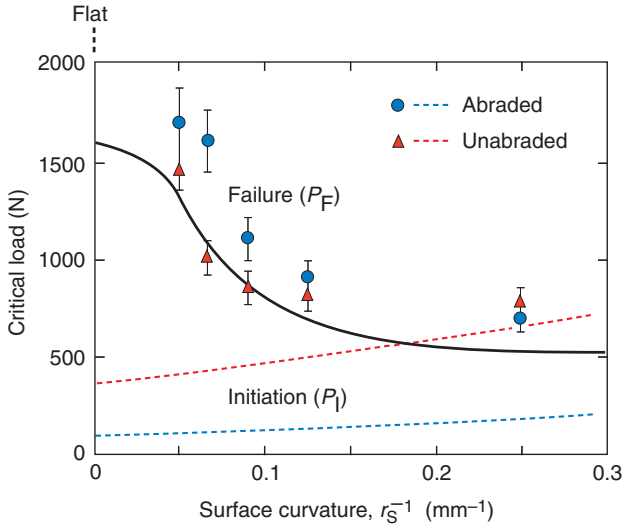

Fig. 10. Critical load for radial crack instability versus plate curvature r_s^{-1} for glass/epoxy dome bilayers, thickness $d = 1$ mm and inner radius $r_s = 8$ mm. Solid curve is boundary element analysis (BEA)-predicted failure load P_F. Data points are experimental values for abraded and unabraded glass. Dashed curves are BEA-predicted initiation loads for abraded and unabraded glass. After Qasim *et al.*[40,41]

actually rise slightly. Over much of the data range, $P_I << P_F$, meaning that the radial cracks undergo pronounced stable growth before instability. However, for unabraded specimens, the condition $P_I > P_F$ can be achieved in highly curved specimens, in which case the radial cracks, once initiated, go spontaneously and catastrophically to failure.

In certain circumstances, dome structures may become more susceptible to cracks initiating from the margins rather than from directly under the indenter. Such cracks are indicated as L cracks in Fig. 7(a). This state of affairs is enhanced in loading with ultra-compliant indenters, and in specimens with edge damage.[52] Such indenter materials may be considered to resemble some of the properties of food bolus in chewing.[4,19] The chief outcomes of soft contacts are twofold: first diminish the stress intensity beneath the contact; and second displace the tensile stress maxima toward the dome margins. Off-axis loading exacerbates this latter outcome by locating the load axis closer to

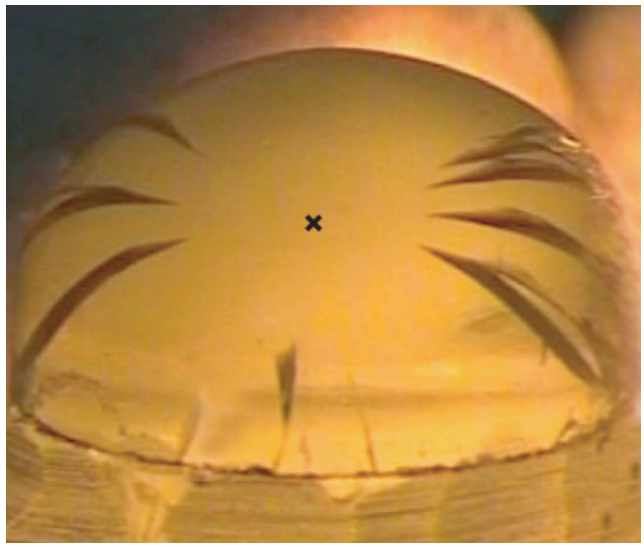

Fig. 11. Front-on view of off-axis contact fracture of epoxy-filled glass domes, $d = 1$ mm and $r_s = 6$ mm, on epoxy base. Indentation with teflon disk at 1000 N. Note how margin cracks initiate and propagate around side of dome toward contact center (cross) to form "tiger" pattern. Courtesy Mahek M Shah and Vibhu P Saxena.

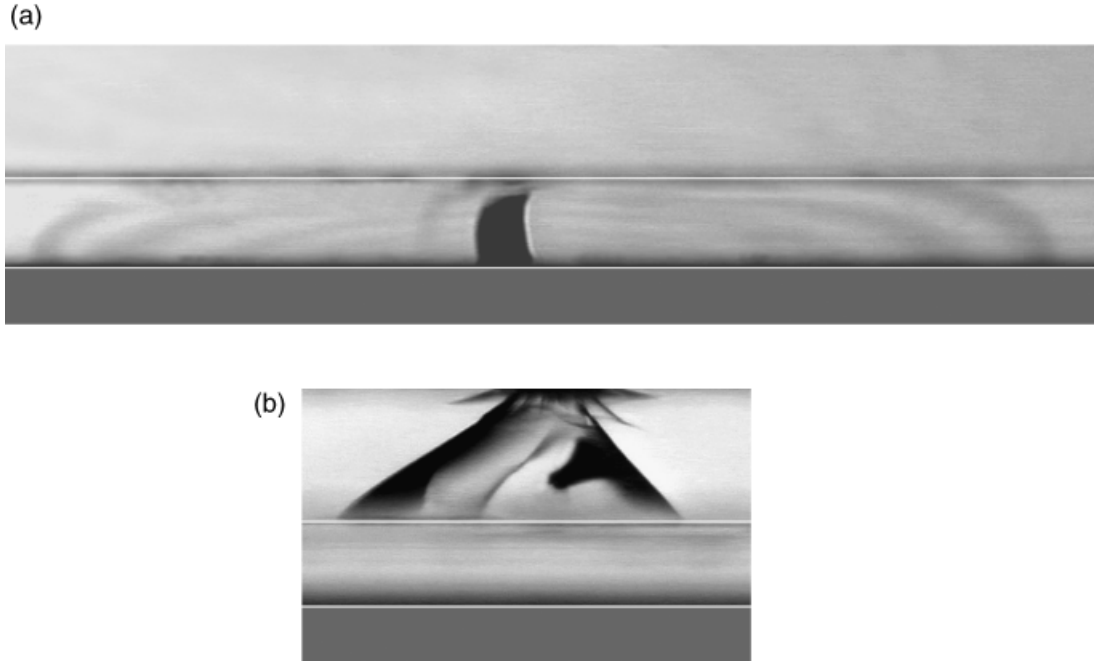

Fig. 12. Failure in epoxy-bonded glass/sapphire/polycarbonate trilayers, $d_v = 1$ mm and $d_c = 0.5$ mm, from contact with tungsten carbide spheres of radius $r = 5.0$ mm, frequency 10 Hz. (a) Core R crack in bottom-surface abraded sapphire, at $P_m = 400$ N and $n_F = 1014$ cycles. Initiation and layer penetration occur simultaneously. (b) Veneer I crack in top-surface abraded glass layer, at $P_m = 300$ N and $n_F = 43\,613$ cycles. Crack evolution after initiation in this case is stable and incremental. (Interfaces accentuated by superimposed white lines for clarity.) After Bhowmick *et al.*[53]

the dome edge.[47] An example of margin fractures generated by an off-axis flat teflon indenter is shown in Fig. 11. In this case cracks have spread from the extremities, and are seen converging to the point of contact (marked by cross) to form a "tiger" pattern. The coalescence of such cracks produces spalls reminiscent of the lunar fractures referred to in Fig. 1(c).

III. Trilayers

(1) Model Tests

As indicated in the Introduction, most all-ceramic crowns consist of an esthetic but weak porcelain veneer joined onto a strong and stiff ceramic core. The two most widely used ceramic core materials are alumina and zirconia based (although glass ceramics are also used in some cases). Alumina is stiffer, providing more support and stress shielding for the veneer (as well as for the substrate), but is weaker and thus susceptible to core failure[27,34]; zirconia is stronger, and therefore less liable to core failure. The primary fracture modes are the same as for bilayers, but the system is now also vulnerable to delamination at the veneer/core interface as well as to radial cracking in the veneer.

All-transparent model trilayer systems are readily fabricated as before, but with a model transparent sapphire core layer inserted between the glass veneer and polycarbonate substrate.[27,34,45] In its simplest form, the glass is epoxy-bonded onto the core. Provided the epoxy is thin enough (<20 μm), the system is relatively immune to residual stresses from shrinkage and from flexural failure of the veneer.[23] Moreover, the bond is sufficiently strong that delamination again does not constitute a primary mode of failure. Figure 12 shows cracks in such a model system with veneer and core thicknesses $d_v = 1.0$ mm and $d_c = 0.5$ mm, subjected to cyclic contact loading in water. An abrasion treatment has been given to the sapphire bottom surface in Fig. 12(a), to the glass top surface in Fig. 12(b). The cracks are analogous to those seen in Fig. 3 for glass/polycarbonate bilayers. Again, failure is defined as penetration through the layer, in this case to the veneer/core interface. However, a notable difference in the manner of failure now becomes apparent—the radial crack shows no steady evolution through the core layer, but pops abruptly to the interface at initiation, with exaggerated radial propagation (the latter reflecting a release of excess flexural energy stored in the stiff core layer). This result simplifies analysis of failure of systems with opaque ceramic cores, as failure may be equated with first appearance of radial cracking by subsurface viewing through the substrate.[34] On the other hand, the cone crack shows the usual steady, incremental growth through the veneer. With increased loading or extended cycling, the arrested radial crack may eventually reinitiate in the adjacent weak veneer layer, as in Fig. 13(a), ultimately

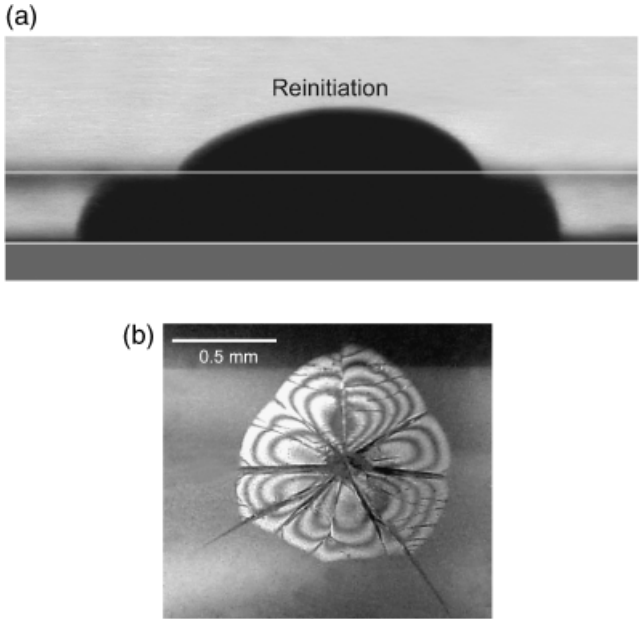

Fig. 13. Subsidiary fracture modes in same system as in Fig. 12 after extended cycling at $P_m = 375$ N. (a) Reinitiation in adjacent, bottom-surface abraded, glass veneer layer, after $n = 4129$ cycles. (b) Delamination at interface, after $n = 3261$ cycles (note how pattern is constrained by preceding radials). After Bhowmick *et al.*[53]

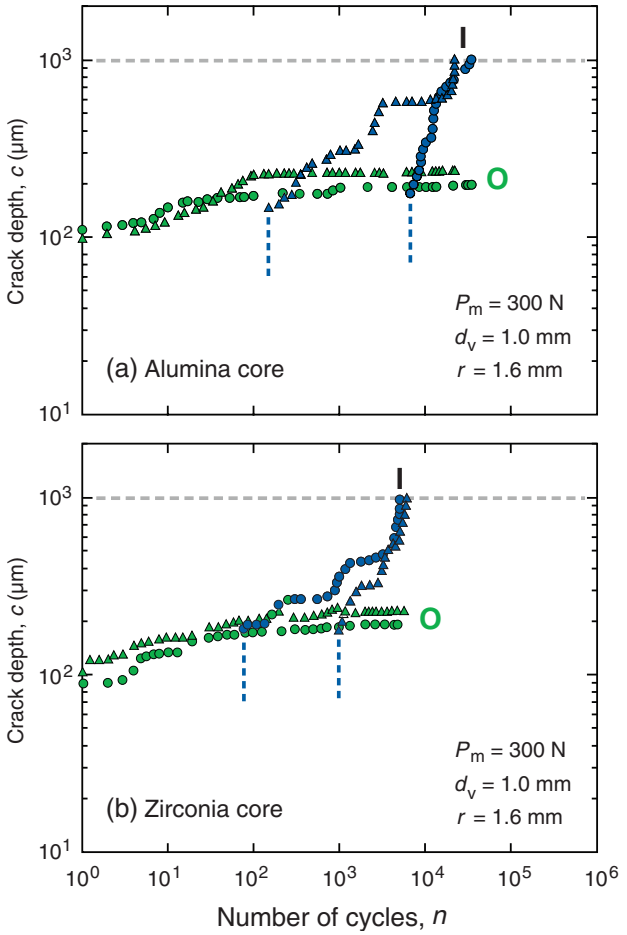

Fig. 14. Cone crack depth c for trilayers of top-surface-abraded glass, $d_v = 1.0$ mm (dashed lines), epoxy-bonded onto (a) alumina and (b) zirconia cores, $d_c = 0.5$ mm, for indentation with tungsten carbide sphere radius $r = 1.6$ mm at peak load $P_m = 300$ N, frequency 1 Hz, in water. Each symbol represents a separate test. After Bhowmick *et al.*[53]

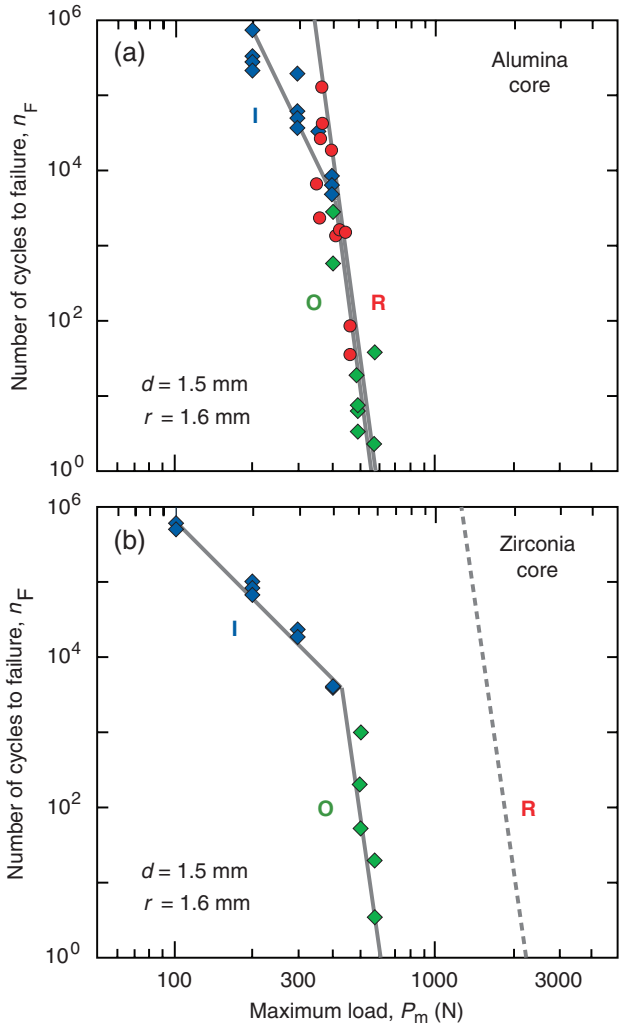

Fig. 15. Number of cycles n_F to contact-induced veneer failure from O and I cone cracks versus core failure from radial R cracks, for glass veneers epoxy-bonded onto (a) alumina and (b) zirconia cores, as function of maximum contact load P_m for tungsten carbide sphere radius $r = 1.6$ mm, frequency 1 Hz, in water. Lines through O and R data in accordance with Eqs. (7) and (8) in Sidebar 1, based on fatigue exclusively by moisture-assisted slow crack growth. Lines through I data are empirical fits. After Bhowmick *et al.*[53]

penetrating the entire "crown," or delaminate at the epoxy-bonded veneer/core interface, as in Fig. 13(b). By contrast, the cone crack does not penetrate into the tough core sublayer, but again delaminates the interface.[46]

The steady evolution of cone cracks in a similar trilayer system with abraded glass veneer but now with (a) alumina and (b) zirconia polycrystalline ceramic cores is quantified in the $c(n)$ data of Fig. 14, for contact at peak load $P_m = 300$ N and sphere radius $r = 1.6$ mm, in water.[53] Prolonged crack propagation before failure is evident for both cone modes (cf. bilayer data, Fig. 5(a)). Again, inner (I) cone cracks, despite a sluggish start, overtake their outer (O) crack counterparts and are responsible for failure. Note that slightly longer lifetimes are realized for the specimens with alumina core, attesting to superior shielding associated with the stiffer ceramic.

The dominance of inner cone cracks evident in Fig. 14 is not universal. This is illustrated by the "failure map" in Fig. 15 for the same epoxy-bonded trilayers.[53] This figure plots the number of cycles n_F for failure, i.e., the first crack to reach the veneer/core interface, as a function of peak cyclic load P_m. In this example, both glass top surface and ceramic bottom surface have been abraded to equalize the flaw conditions in the veneer and core. For alumina cores, Fig. 15(a), the cone and radial modes are truly competitive. In the low-cycle, high-load region, O and R cracks appear equally likely to cause failure. In the high-cycle, low-load region, I cracks begin to dominate. For zirconia cores, Fig. 15(b), the issue seems to be more clear cut—cone cracks are dominant over the entire cycle range, and are a little easier to generate than with alumina cores—radial cracks are more strongly inhibited, and in fact are difficult to initiate before cone crack failure (hence dashed line, indicating prediction only). Interpretation of the zirconia data is complicated by the introduction of abrasion-induced surface compression stresses from phase transformations, which act to suppress all forms of fracture.[37,62,63] Fracture mechanics relations based exclusively on fatigue by moisture-assisted slow crack growth (Sidebar 1) are able to account for the broad features of the O and R data (solid lines), notably a slope $-1/N$ (N = crack velocity exponent) and a shift to the right for the zirconia R data.[53] (Again, analogous relations for I cracks are not available owing to the complexity of the superposed hydraulic pumping mechanism.) Such equations also provide a capacity for predicting relative shifts in data with changes in geometrical variables, notably core material properties and net layer thickness d.

(2) Some Clinical Issues

One issue emerging as a concern in the dental community is that of residual stresses from fabrication processes.[65,66] We have used epoxy to bond our veneer/core interfaces to avoid such stresses. However, although delamination is not a primary mode of failure in our experiments, epoxy is nevertheless a relatively weak interface and unlikely to find usage as a joining process in crown fabrication. The bulk of crown veneering is achieved by fusing

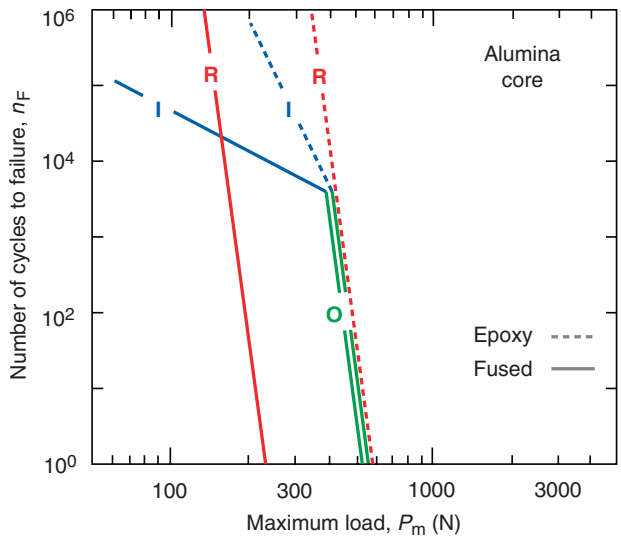

Fig. 16. As for Fig. 15, but for fused (solid) and epoxy-bonded (dashed) glass/alumina interfaces. Shifts are attributable to introduction of residual stresses into fused layers. Data omitted, for clarity. After Bhowmick *et al.*[53]

porcelain onto the ceramic core, and much consideration goes into selecting the right porcelains to minimize coefficient of thermal expansion (CTE) mismatch. This is not always easy to do, because CTE differentials $<1 \times 10^{-6}$ K^{-1} can produce stresses in excess of 50 MPa, depending on the ceramic.[45] Such stresses have long been appreciated in the manufacture of porcelain-fused-to-metal crowns—in that case, higher-contraction metals effectively place the porcelain in compression. In all-ceramic crowns where all components are brittle, CTE stresses can be deleterious to both veneer and core, in which case close matching is highly desirable. To illustrate, Fig. 16 shows design maps for the same system as in Fig. 15(a), but with the glass veneer fused to the alumina core with glass tape at 600°C.[50] The CTE mismatch in this case is estimated at just 2×10^{-6} K^{-1}. Solid lines represent the fused system, dashed lines the epoxy-bonded system (from Fig. 15(a)). It is apparent that residual stress effects can result in substantial reductions in lifetimes.

Another issue that causes a certain consternation in the dental community is the use of hard metal spheres in the indentation testing protocols described here. WC spheres are used primarily as an economic expedient, to minimize damage accumulation in the indenters themselves, especially in long-term cyclic loading. It is argued that true occlusal contacts are made with materials of like modulus (tooth enamel on crown porcelain). Indenter size is also an issue—how does the choice of indenter radius r influence the mechanics? In fact, tests with a broad range of indenter materials and geometries, sphere or flat, shows little change in fracture mode.[52] (An exception is when the indenter modulus E_i becomes very much lower than the veneer modulus E_v for curved specimens, resulting in the switch to margin cracks seen in Fig. 11.) Nor do these variables have much influence on the $n_F(P_m)$ functions in Fig. 15, especially for R cracks, as failure is determined within the contact far field. However, they do have some influence on the critical loads P_I to initiate cone cracks, as demonstrated in Fig. 17 for O crack initiation in glass/alumina/polycarbonate for single-cycle loading: (a) as a function of E_i for fixed indenter size r, (b) as a function of r for fixed indenter modulus E_i.[49] Symbols indicate data points, solid lines theoretical predictions (Eq. (3) in Sidebar 1). Horizontal dashed lines indicate failure loads (e.g., intersection points at $n = 1$ for O-crack data in Fig. 15). Note the condition $P_I > P_F$ in the extreme regions of ultra-low E_i (Fig. 17(a)) and ultra-high r (Fig. 17(b)), corresponding to spontaneous high-load failure.

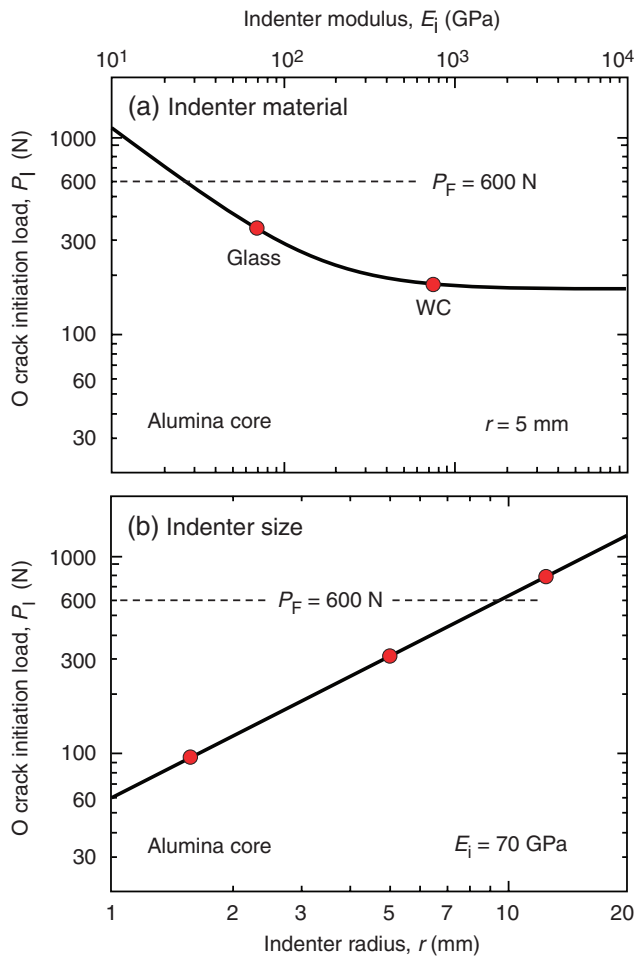

Fig. 17. Critical loads P_I to initiate O cone cracks in glass layer in single-cycle loading calculated from in Eq. (1): (a) as function of indenter modulus E_i, at fixed radius $r = 5.0$ mm; (b) as function of r, at fixed $E_i = 70$ GPa. Dashed lines at $P_F = 600$ N indicate failure load. After Bhowmick *et al.*[49]

IV. What Can We Tell the Dentists?

The work described here bears on several issues that a materials scientist might imagine should be of interest to the dental community in relation to all-ceramic crowns. We enumerate some of these below:

(i) *Failure modes.* We have described several failure modes that may generate in crown-like dome structures, each of which may dominate under different conditions. These include near-contact cone cracking in porcelain veneer layers and radial cracking in the ceramic cores. Lunar-like cracks may initiate at the dome margins. Other modes may also operate in some cases, although most may be considered secondary in the case of all-ceramic crown systems: delaminations at veneer/core or core/dentin interfaces; radial cracks at the bottom of the veneer rather than core layer when bonded to the core with a relatively thick, compliant adhesive,[23,35] or fused onto a soft metal core;[29,33] median cracks in quasiplastic ceramics.[43,58,59] It is little wonder then that controversy persists in the dental literature concerning initiation sites for crown failure—the complex geometry makes it difficult to measure thicknesses at all points of the crown, and there is no accurate clinical history of loading conditions. Early cracks or chips may be ignored by the patient, and additional fractures may occur before the clinician is made aware of any problems.

(ii) *Fatigue.* All ceramics are susceptible to fatigue in cyclic contact loading, especially in aqueous environments.[59,67] With outer cone cracks and radial cracks, fatigue is modest, attributable to slow crack growth over integrated time of occlusal contact. Inner cone cracks are especially susceptible, owing to the

Sidebar 1. Mechanics of Crack Initiation and Failure

Consider the trilayer structure in Fig. 1. It is convenient to treat two cases of loading separately, single-cycle and multi-cycle loading:

(1) Single-Cycle Loading

Occlusal contact is well simulated by a classical Hertzian contact.[55] For cones, it is only the outer (O) crack that forms in single-cycle loading. In single-cycle loading, crack propagation may, to first approximation, be assumed to occur under equilibrium conditions of fracture. The critical loads P_I to initiate an O crack in the veneer surface and P_F to propagate it through to the veneer/core interface have the form[38,43,45]

$$P_I = A\kappa r T v^2 / E_v \tag{3}$$

$$P_F = C\lambda T_v d_v^{3/2} \tag{4}$$

where $\boldsymbol{T}$ is toughness ($\boldsymbol{K}_{IC}$), $\boldsymbol{\kappa} = \boldsymbol{\kappa}(\boldsymbol{E}_i/\boldsymbol{E}_v)$ and $\boldsymbol{\lambda} = \boldsymbol{\lambda}(\boldsymbol{E}_s/\boldsymbol{E}_c, \boldsymbol{E}_v/\boldsymbol{E}_c, \boldsymbol{d}_v/\boldsymbol{d}_c)$ are slowly varying functions of relative indenter (i) plus veneer (v) and core (c) properties. Note the dependence on $\boldsymbol{r}$ in Eq. (3) (see Fig. 16(b)), as initiation is determined by the near-contact field, and on $\boldsymbol{d}_v$ in Eq. (4), as failure is governed by the distance the crack propagates through the veneer. (However, the $\boldsymbol{d}_v$ dependence in Eq. (4) is likely to be weaker than indicated here, because of counteracting effects in the $\boldsymbol{\lambda}$ term, among other things.) Veneer toughness appears as the main material parameter because both initiation and propagation of the cone crack involve a precursor stable growth phase before instability. Moduli of the layer materials and the indenter are also factors (see Fig. 16(a)). Most commonly, $\boldsymbol{P}_I < \boldsymbol{P}_F$, so the crack grows steadily through the veneer with increasing load. In the extreme of very large $\boldsymbol{r}/\boldsymbol{d}$, the condition $\boldsymbol{P}_I > \boldsymbol{P}_F$ may be satisfied, in which case initiation leads spontaneously to failure.

For radial (R) cracks, failure is determined primarily by the flexural component of the applied stress field, and occurs spontaneously at initiation[28,34]

$$P_F = P_I = BS_c d^2 (E_*/E_c)/\log(E_*/E_s) \tag{5}$$

where S_c is the strength of the core, B is a coefficient, and $E_* = E_*(E_s/E_c, E_v/E_c, d_v/d_c)$ is an effective modulus for the composite veneer/core bilayer ($E_* = E_v = E_c$ for bilayers).[34] Again, the failure load depends on d and not on r. Note in this case that it is the strength of the core that governs the failure, because initiation under equilibrium conditions is assumed to occur spontaneously from a critical flaw without any precursor extension. Again, relative layer (but not indenter) modulus is a factor.

(2) Cyclic Loading

Under cyclic conditions, the cracks can grow with time. In its simplest manifestation, fatigue in ceramics occurs by slow crack growth, as described by a crack velocity equation $\boldsymbol{v} \sim (\mathrm{K}/\mathrm{T})^{\boldsymbol{N}}$, where K is a stress intensity factor and N is a velocity exponent.[64] As indicated in the text, this appears to be the mode of fatigue governing O and R cracks. The governing equations for the number of cycles to initiate O cracks and to take them to failure are of the simple power-law form

$$n_I = (P_I/P_m)^{N/2} \tag{6}$$

$$n\mathrm{F} = (P_F/P_m)N \tag{7}$$

For R cracks, initiation and failure are again simultaneous

$$n_F = n_I = (P_F/P_m)^N \tag{8}$$

which has the same form as Eq. (7).

Cyclic loading in water also generates inner (I) cone cracks. For these, the analysis is more complex, owing to the superposition of hydraulic pumping onto slow crack growth.[39,57] Relations analogous to 3–8 have not been obtained.

superposition of hydraulic pumping onto the slow growth mechanism. Clinicians should therefore not rely on fracture data from the usual "standardized" test specimens (notably bend bars) in single-cycle loading in ambient laboratory atmosphere for materials evaluation.

(iii) *Fatigue versus single-cycle overload failure*. Is crown failure more likely to occur from cumulative damage over many cycles or from a single overload biting event? In the design maps of Figs. 15 or 17, single-cycle overload is equivalent to translating along the horizontal axis $n = 1$, in which case fracture occurs exclusively from O or R cracks at a relatively high bite force. Fatigue failure is equivalent to translating along a vertical line P_m = constant at lower loads, bringing the deleterious I cracks into play. Both of these loading conditions may be active in ordinary oral function.

(iv) *Which materials?* The fracture mechanics (Sidebar 1) suggest the following optimal material properties: for the core—a ceramic of high strength (resist radial fracture) and high modulus (optimize stress shielding); for the veneer—a porcelain of moderate toughness (resist cone crack growth) and high hardness (resist quasiplasticity).

(v) *Geometrical properties*. Minimize cuspal curvatures and net crown thicknesses, as much as allowable within the constraints of remaining tooth and adjacent dentition. Critical loads for fracture are less sensitive to relative veneer/core thicknesses.[34]

(vi) *Surface preparation*. To preserve strength of veneer and core materials, minimize surface abrasion in crown preparation, e.g., finishing by sandblasting or crown adjustment with burrs, especially in the vulnerable near-contact and margin areas.[48]

(vii) *CTE mismatch*. Residual tensile stresses from CTE mismatch can be highly deleterious, affecting both veneer and core. Judicious selection of materials with small mismatch to introduce compressive stresses is an option mooted by some researchers, but it is important to note that compression in one part of the system must always be counterbalanced by tension elsewhere.

Acknowledgments

Contributions to this research program by many colleagues, too numerous to list here, are gratefully acknowledged. We also wish to thank Dr. S. S. Scherrer and Prof. K. A. Malament for providing the photographs in Fig. 1.

Certain equipment, instruments or materials are identified in this paper in order to specify experimental details. Such identification does not imply recommendation by the National Institute of Standards and Technology.

References

[1]B. R. Lawn, "Ceramic-Based Layer Structures for Biomechanical Applications," *Curr. Opin. Solid State Mater. Sci.*, **6** [3] 229–35 (2002).

[2]B. R. Lawn, Y. Deng, P. Miranda, A. Pajares, H. Chai, and D. K. Kim, "Overview: Damage in Brittle Layer Structures From Concentrated Loads," *J. Mater. Res.*, **17** [12] 3019–36 (2002).

[3]B. R. Lawn, A. Pajares, Y. Zhang, Y. Deng, M. Polack, I. K. Lloyd, E. D. Rekow, and V. P. Thompson, "Materials Design in the Performance of All-Ceramic Crowns," *Biomaterials*, **25** [14] 2885–92 (2004).

[4]J. W. McLean, *The Science and Art of Dental Ceramics. Vol. 1: The Nature of Dental Ceramics and Their Clinical Use*. Quintessence, Chicago, 1979.

[5]S. S. Scherrer and W. G. deRijk, "The Fracture Resistance of All-Ceramic Crowns on Supporting Structures With Different Elastic Moduli," *Int. J. Prosthodont.*, **6** [5] 462–7 (1993).

[6]W. P. Kelsey, T. Cavel, R. J. Blankenau, W. W. Barkmeier, T. M. Wilwerding, and M. A. Latta, "4-Year Clinical Study of Castable Ceramic Crowns," *Am. J. Dent.*, **8** [5] 259–62 (1995).

[7]M. Fradeani and A. Aquilano, "Clinical Experience With Empress Crowns," *Int. J. Prosthodont.*, **10** [3] 241–7 (1997).

[8]J. R. Kelly, "Ceramics in Restorative and Prosthetic Dentistry," *Ann. Rev. Mater. Sci.*, **27**, 443–68 (1997).

[9]K. J. Anusavice and Y. L. Tsai, "Stress Distribution in Ceramic Crown Forms as a Function of Thickness, Elastic Modulus, and Supporting Substrate"; pp. 264–7 in *Proceedings of the Sixteenth Southern Biomedical Engineering Conference*, Edited by J. D. Bumgardner, and A. D. Puckett. Biloxi , MS, 1997.

[10]J. R. Kelly, "Clinically Relevant Approach to Failure Testing of All-Ceramic Restorations," *J. Prosthet. Dent.*, **81** [6] 652–61 (1999).

[11]G. Sjogren, R. Lantto, and A. Tillberg, "Clinical Evaluation of All-Ceramic Crowns (Dicor) in General Practice," *J. Prosthet. Dent.*, **81** [3] 277–84 (1999).

[12]G. Sjogren, R. Lantto, A. Granberg, B. O. Sundstrom, and A. Tillberg, "Clinical Examination of Leucite-Reinforced Glass–Ceramic Crowns (Empress) in General Practice: A Retrospective Study," *Int. J. Prosthodont.*, **12** [2] 122–8 (1999).

[13]K. A. Malament and S. S. Socransky, "Survival of Dicor Glass–Ceramic Dental Restorations Over 14 years: I. Survival of Dicor Complete Coverage Restorations and Effect of Internal Surface Acid Etching, Tooth Position, Gender and Age," *J. Prosthet. Dent.*, **81** [1] 23–32 (1999).

[14]K. A. Malament and S. S. Socransky, "Survival of Dicor Glass–Ceramic Dental Restorations Over 14 years: II. Effect of Thickness of Dicor Material and Design of Tooth Preparation," *J. Prosthet. Dent.*, **81** [6] 662–7 (1999).

[15]K. A. Malament and S. S. Socransky, "Survival of Dicor Glass–Ceramic Dental Restorations Over 16 years: Part III: Effect of Luting Agent and Tooth or Tooth-Substitute Core Structure," *J. Prosthet. Dent.*, **86** [5] 511–9 (2001).

[16]E. A. McLaren and S. N. White, "Survival of In-Ceram Crowns in a Private Practice: A Prospective Clinical Trial," *J. Prosthet. Dent.*, **83** [2] 216–22 (2000).

[17]M. Fradeani and M. Redemagni, "An 11-Year Clinical Evaluation of Leucite-Reinforced Glass–Ceramic Crowns: A Retrospective Study," *Quintessence Int.*, **33** [7] 503–10 (2002).

[18]J. R. Kelly, "Dental Ceramics: Current Thinking and Trends," *Dent. Clin. North Am.*, **48** [2] 513–30 (2004).

[19]P. W. Lucas, *Dental Functional Morphology: How Teeth Work*. Cambridge University Press, Cambridge, UK, 2004.

[20]A. Oden, M. Andersson, I. Krystek-Ondracek, and D. Magnusson, "Five-year Clinical Evaluation of Procera AllCeram Crowns," *J. Prosthet. Dent.*, **80** [4] 450–6 (1998).

[21]Y. G. Jung, S. Wuttiphan, I. M. Peterson, and B. R. Lawn, "Damage Modes in Dental Layer Structures," *J. Dent. Res.*, **78** [4] 887–97 (1999).

[22]H. Chai, B. R. Lawn, and S. Wuttiphan, "Fracture Modes in Brittle Coatings With Large Interlayer Modulus Mismatch," *J. Mater. Res.*, **14** [9] 3805–17 (1999).

[23]H. Chai and B. R. Lawn, "Role of Adhesive Interlayer in Transverse Fracture of Brittle Layer Structures," *J. Mater. Res.*, **15** [4] 1017–24 (2000).

[24]K. S. Lee, Y.-W. Rhee, D. H. Blackburn, B. R. Lawn, and H. Chai, "Cracking of Brittle Coatings Adhesively Bonded to Substrates of Unlike Modulus," *J. Mater. Res.*, **15** [8] 1653–6 (2000).

[25]H. Zhao, X. Z. Hu, M. B. Bush, and B. R. Lawn, "Contact Damage in Porcelain/Pd-Alloy Bilayers," *J. Mater. Res.*, **15** [3] 676–82 (2000).

[26]B. R. Lawn, Y. Deng, and V. P. Thompson, "Use of Contact Testing in the Characterization and Design of All-Ceramic Crown-Like Layer Structures: A Review," *J. Prosthet. Dent.*, **86** [5] 495–510 (2001).

[27]P. Miranda, A. Pajares, F. Guiberteau, F. L. Cumbrera, and B. R. Lawn, "Contact Fracture of Brittle Bilayer Coatings on Soft Substrates," *J. Mater. Res.*, **16** [1] 115–26 (2001).

[28]Y.-W. Rhee, H.-W. Kim, Y. Deng, and B. R. Lawn, "Contact-Induced Damage in Ceramic Coatings on Compliant Substrates: Fracture Mechanics and Design," *J. Am. Ceram. Soc.*, **84** [5] 1066–72 (2001).

[29]H. Zhao, X. Hu, M. B. Bush, and B. R. Lawn, "Cracking of Porcelain Coatings Bonded to Metal Substrates of Different Modulus and Hardness," *J. Mater. Res.*, **16** [5] 1471–8 (2001).

[30]Y. Deng, B. R. Lawn, and I. K. Lloyd, "Characterization of Damage Modes in Dental Ceramic Bilayer Structures," *J. Biomed. Mater. Res.*, **63B** [2] 137–45 (2002).

[31]B. R. Lawn, Y. Deng, I. K. Lloyd, M. L. Janal, E. D. Rekow, and V. P. Thompson, "Materials Design of Ceramic-Based Layer Structures for Crowns," *J. Dent. Res.*, **81** [16] 433–8 (2002).

[32]C.-S. Lee, D. K. Kim, J. Sanchez, P. Miranda, A. Pajares, and B. R. Lawn, "Rate Effects in Critical Loads for Radial Cracking in Ceramic Coatings," *J. Am. Ceram. Soc.*, **85** [8] 2019–24 (2002).

[33]H. Zhao, P. Miranda, B. R. Lawn, and X. Hu, "Cracking in Ceramic/Metal/Polymer Trilayer Systems," *J. Mater. Res.*, **17** [5] 1102–11 (2002).

[34]Y. Deng, P. Miranda, A. Pajares, F. Guiberteau, and B. R. Lawn, "Fracture of Ceramic/Ceramic/Polymer Trilayers for Biomechanical Applications," *J. Biomed. Mater. Res.*, **67A** [3] 828–33 (2003).

[35]J. H. Kim, P. Miranda, D. K. Kim, and B. R. Lawn, "Effect of an Adhesive Interlayer on the Fracture of a Brittle Coating on a Supporting Substrate," *J. Mater. Res.*, **18** [1] 222–7 (2003).

[36]Y. Zhang and B. R. Lawn, "Long-Term Strength of Ceramics for Biomedical Applications," *J. Biomed. Mater. Res.*, **69B** [2] 166–72 (2004).

[37]Y. Zhang, B. R. Lawn, E. D. Rekow, and V. P. Thompson, "Effect of Sandblasting on the Long-Term Strength of Dental Ceramics," *J. Biomed. Mater. Res.*, **71B** [2] 381–6 (2004).

[38]S. Bhowmick, Y. Zhang, and B. R. Lawn, "Competing Fracture Modes in Brittle Materials Subject to Concentrated Cyclic Loading in Liquid Environments: Bilayer Structures," *J. Mater. Res.*, **20** [10] 2792–800 (2005).

[39]H. Chai and B. R. Lawn, "Hydraulically Pumped Cone Fractures in Brittle Solids," *Acta Mater.*, **53**, 4237–44 (2005).

[40]T. Qasim, M. B. Bush, X. Hu, and B. R. Lawn, "Contact Damage in Brittle Coating Layers: Influence of Surface Curvature," *J. Biomed. Mater. Res.*, **73B** [1] 179–85 (2005).

[41]M. Rudas, T. Qasim, M. B. Bush, and B. R. Lawn, "Failure of Curved Brittle Layer Systems from Radial Cracking in Concentrated Loading," *J. Mater. Res.*, **20** [10] 2812–9 (2005).

[42]Y. Zhang, J.-K. Kwang, and B. R. Lawn, "Deep Penetrating Conical Cracks in Brittle Layers From Hydraulic Cyclic Contact," *J. Biomed. Mater. Res.*, **73B** [1] 186–93 (2005).

[43]Y. Zhang, S. Bhowmick, and B. R. Lawn, "Competing Fracture Modes in Brittle Materials Subject to Concentrated Cyclic Loading in Liquid Environments: Monoliths," *J. Mater. Res.*, **20** [8] 2021–9 (2005).

[44]S. Bhowmick, V. Jayaram, and S. K. Biswas, "Deconvolution of Fracture Properties of TiN Films on Steels From Nanoindentation Load–Displacement Curves," *Acta Mater.*, **53**, 2459–67 (2005).

[45]I. Hermann, S. Bhowmick, Y. Zhang, and B. R. Lawn, "Competing Fracture Modes in Brittle Materials Subject to Concentrated Cyclic Loading in Liquid Environments: Trilayer Structures," *J. Mater. Res.*, **21** [2] 512–21 (2006).

[46]J.-W. Kim, S. Bhowmick, I. Hermann, and B. R. Lawn, "Transverse Fracture of Brittle Layers: Relevance to Failure of All-Ceramic Dental Crowns," *J. Biomed. Mater. Res.*, **79B** [1] 58–65 (2006).

[47]T. Qasim, C. Ford, M. B. Bush, X. Hu, and B. R. Lawn, "Effect of Off-Axis Concentrated Loading on Failure of Curved Brittle Layer Structures," *J. Biomed. Mater. Res.*, **76B** [2] 334–9 (2006).

[48]Y. Zhang, B. R. Lawn, K. A. Malament, V. P. Thompson, and E. D. Rekow, "Damage Accumulation and Fatigue Life of Particle-Abraded Dental Ceramics," *Int. J. Prosthodont.*, **19** [5] 442–8 (2006).

[49]S. Bhowmick, J. J. Meléndez-Martínez, I. Herman, Y. Zhang, and B. R. Lawn, "Role of Indenter Material and Size in Veneer Failure of Brittle Layer Structures," *J. Biomed. Mater. Res.* (in press).

[50]I. Hermann, S. Bhowmick, and B. R. Lawn, "Role of Core Support Material in Veneer Failure of Brittle Layer Structures," *J. Biomed. Mater. Res.* (in press).

[51]J.-W. Kim, S. Bhowmick, H. Chai, and B. R. Lawn, "Role of Substrate Material in Failure of Crown-Like Layer Structures," *J. Biomed. Mater. Res.* (in press).

[52]T. Qasim, C. Ford, M. B. Bush, X. Hu, K. A. Malament, and B. R. Lawn, "Margin Failures in Brittle Dome Structures: Relevance to Failure of Dental Crowns," *J. Biomed. Mater. Res.*, **80B** [1] 78–85 (2007).

[53]S. Bhowmick, J. J. Meléndez-Martínez, Y. Zhang, and B. R. Lawn, "Design Maps for Failure of All-Ceramic Layer Structures in Concentrated Cyclic Loading," *Acta Mater.*, (in press).

[54]B. R. Lawn, K. S. Lee, H. Chai, A. Pajares, D. K. Kim, S. Wuttiphan, I. M. Peterson, and X. Hu, "Damage-Resistant Brittle Coatings," *Adv. Eng. Mater.*, **2** [11] 745–8 (2000).

[55]B. R. Lawn, "Indentation of Ceramics With Spheres: A Century After Hertz," *J. Am. Ceram. Soc.*, **81** [8] 1977–94 (1998).

[56]Y. Zhang, A. Pajares, and B. R. Lawn, "Fatigue and Damage Tolerance of Y-TZP Ceramics in Layered Biomechanical Systems," *J. Biomed. Mater. Res.*, **71B** [1] 166–71 (2005).

[57]H. Chai and B. R. Lawn, "Hydraulically Pumped Cone Fracture in Bilayers With Brittle Coatings," *Script. Mater.*, **55**, 343–6 (2006).

[58]F. Guiberteau, N. P. Padture, H. Cai, and B. R. Lawn, "Indentation Fatigue: A Simple Cyclic Hertzian Test for Measuring Damage Accumulation in Polycrystalline Ceramics," *Philos. Mag.*, **A 68** [5] 1003–16 (1993).

[59]Y.-G. Jung, I. M. Peterson, D. K. Kim, and B. R. Lawn, "Lifetime-Limiting Strength Degradation From Contact Fatigue In Dental Ceramics," *J. Dent. Res.*, **79** [2] 722–31 (2000).

[60]A. Abdul-Baqi and E. v. d. Giessen, "Numerical Analysis of Indentation-Induced Cracking of Brittle Coatings on Ductile Substrates," *Int. J. Solids Struct.*, **39**, 1427–42 (2002).

[61]P. Miranda, A. Pajares, F. Guiberteau, Y. Deng, and B. R. Lawn, "Designing Damage-Resistant Brittle-Coating Structures: I. Bilayers," *Acta Mater.*, **51** [14] 4347–56 (2003).

[62]T. Kosmac, C. Oblak, P. Jevnikar, N. Funduk, and L. Marion, "The Effect of Surface Grinding and Sandblasting on Flexural Strength and Reliability of Y-TZP Zirconia Ceramic," *Dent. Mater.*, **15**, 426–33 (1999).

[63]T. Kosmac, C. Oblak, P. Jevnikar, N. Funduk, and L. Marion, "Strength and Reliability of Surface Treated Y-TZP Dental Ceramics," *J. Biomed. Mater. Res.*, **53** [4] 304–13 (2000).

[64]S. M. Wiederhorn and L. H. Bolz, "Stress Corrosion and Static Fatigue of Glass," *J. Am. Ceram. Soc.*, **53** [10] 543–8 (1970).

[65]B. Taskonak, J. J. Mecholsky, and K. J. Anusavice, "Residual Stresses in Bilayer Dental Ceramics," *Biomaterials*, **26**, 3235–41 (2005).

[66]G. Isgro, H. Wang, C. J. Kleverlaan, and A. J. Feilzer, "The Effects of Thermal Mismatch and Fabrication Procedures on the Deflection of Layered All-Ceramic Discs," *Dent. Mater.*, **21** [7] 649–55 (2005).

[67]D. K. Kim, Y.-G. Jung, I. M. Peterson, and B. R. Lawn, "Cyclic Fatigue of Intrinsically Brittle Ceramics in Contact With Spheres," *Acta Mater.*, **47** [18] 4711–25 (1999). □

Brian Lawn obtained B.Sc. and Ph.D. degrees in Physics at the University of Western Australia in 1959 and 1963, respectively. After graduating, he spent 4 years as a Postdoctoral Fellow at the University of Bristol and at Brown University. From 1968 Dr. Lawn held a professorial position in Applied Physics at the University of New South Wales. In 1981 Dr. Lawn joined the National Institute of Standards and Technology, and in 1987 was appointed to the position of NIST Fellow. He has held Adjunct Professor appointments at Lehigh and Carnegie Mellon Universities, the University of Maryland, the University of Western Australia, Curtin University, and Xi'an Jiatong University (China). Dr. Lawn has conducted extensive research on the properties of brittle materials, has published over 270 research papers, and is the author of the book "Fracture of Brittle Solids," now in its second edition. In 2001, he was elected a member of the U.S. National Academy of Engineering.

Dianne Rekow earned B.S., B.M.E., M.S.M.E., D.D.S., and Ph.D. degrees and an Orthodontics specialty certificate from the University of Minnesota in 1966, 1982, 1983, 1988, and 1985, respectively, and an MBA from the College of St. Thomas in 1978. After spending 11 years in industry, Dr. Rekow began her academic career following her Ph.D. with appointments at the University of Minnesota (1988–89) as an instructor, University of Maryland (1990–1994) as assistant and associate professor with tenure, and University of Medicine and Dentistry at New Jersey (1994–2002) as professor and chair of the Department of Orthodontics. In 2002 she joined the faculty of New York University College of Dentistry as Director of Translational Research, and in 2006 was appointed Chair of the Department of Basic Science and Craniofacial Biology. Since 1994, Dr. Rekow has lead an NIH-funded program-project team integrating efforts of investigators from the National Institute of Standards and Technology, seven universities, and six corporate partners to investigate damage initiation and propagation in brittle materials, particularly in dental applications. She is a Fellow of the Academy of Dental Materials and the American and International Colleges of Dentists. She is currently President of the American Association for Dental Research.

Mark Bush graduated with a Bachelor of Engineering (Mechanical) with Honours and the University Medal from the University of Queensland in 1979 and then a Ph.D. from the University of Sydney in 1983. His Ph.D. project focused on the development of computational methods for modelling the flow of nonlinear viscous fluids (Rheology). In 1984 he took up the post of Lecturer in Mechanical Engineering at the University of Western Australia and was promoted to Professor in 1998. He has lectured in thermodynamics, fluid mechanics, computational mechanics and materials engineering, and served as Head of the Department of Mechanical and Materials Engineering from 1998 to 2001. He is now Dean of the Faculty of Engineering Computing and Mathematics. He has received awards for both undergraduate teaching and research supervision. He is a Chartered Professional Engineer and Fellow of the Institution of Engineers Australia. His research interests include computational and experimental studies of physical phenomena in both fluid and solid systems. His current research interest is in biomedical materials.

Sanjit Bhowmick received his Bachelor Degree in Metallurgy from the National Institute of Technology, Durgapur in 1997, and ME and Ph.D. in Materials Engineering from the Indian Institute of Science, Bangalore in 2003. His Ph.D. work focused on contact-induced deformation mechanisms in TiN films deposited onto steel substrates. In 2004, he joined Dr. Brian R. Lawn at the National Institute of Standards and Technology as a Guest Researcher. His work at NIST has been on the design of fracture resistant ceramic layers for biomechanical applications. He has published 15 research papers in international journals and presented 12 papers at conferences. His research interests include nanomechanics, processing and characterization of thin films, ceramic layer structures, biomechanical ceramics, and fatigue and fracture.

Tarek Qasim is a Research Fellow in the School of Mechanical Engineering at the University of Western Australia. His research interests include: fracture and fatigue of engineering materials; advanced structural ceramics and composites; fracture mechanics modelling, and finite element analysis (FEA). Dr. Qasim received his Ph.D. with honors from The University of Western Australia in 2006, MS from Tuskegee University in 1986 and BS from the University of Mosul in 1983 (all in Mechanical Engineering). He is a member of the Institute of Engineers Australia, the Jordan Engineering Association, the Australian Research Network for Advanced Materials (Australian Research Council), and a Member of the Community of Science Network in Australia.

Dr. Yu Zhang received his Ph.D. in Materials Science and Engineering from Monash University, Australia. From 2002 to 2005 he worked as a Postdoctoral fellow at the Materials Science and Engineering Laboratory, National Institute of Standards and Technology. In Feb. 2005 Dr. Zhang joined Department of Biomaterials and Biomimetics, New York University College of Dentistry as an Assistant Professor. His current research interests include the development of functionally graded ceramic structures for optimal damage resistance, new ceramic composites for dental and orthopedic applications, and fabrication of Hydroxyapatite-based scaffolds for bone repair.